Biomass-burning particle measurements: Characteristic composition and chemical processing

Paula K. Hudson,[1,2] Daniel M. Murphy,[1] Daniel J. Cziczo,[1,2] David S. Thomson,[1,2] Joost A. de Gouw,[1,2] Carsten Warneke,[1,2] John Holloway,[1,2] Hans-Jürg Jost,[3] and Gerd Hübler[1,2]

Received 28 November 2003; revised 18 February 2004; accepted 23 February 2004; published 1 July 2004.

[1] The NOAA Lockheed Orion WP-3D aircraft intercepted a forest fire plume over Utah on 19 May 2002 during the Intercontinental Transport and Chemical Transformation (ITCT) mission. Large enhancements in acetonitrile (CH_3CN), carbon monoxide (CO) and particle number were measured during the fire plume interception. In the 100 s plume crossing, the Particle Analysis by Laser Mass Spectrometry (PALMS) instrument acquired 202 positive mass spectra from ionizing single particles in the 0.2–5 μm size range. These particles contained carbon, potassium, organics, and ammonium ions. No pure soot particles were sampled directly from the plume. By characterizing these particle mass spectra, a qualitative biomass-burning particle signature was developed that was then used to identify biomass-burning particles throughout ITCT. The analysis was extended to identify biomass-burning particles in four other missions, without the benefit of gas-phase biomass-burning tracers. During ITCT, approximately 33% of the particles sampled in the North American troposphere and 37% of the particles transported from Asia, not influenced by North American sources, were identified as biomass-burning particles. During the WB-57 Aerosol Mission (WAM), Atmospheric Chemistry of Combustion Emissions near the Tropopause (ACCENT) and ACCENT 2000 missions, 7% of stratospheric particles were identified as biomass-burning particles. During the Cirrus Regional Study of Tropical Anvils and Cirrus Layers – Florida Area Cirrus Experiment (CRYSTAL-FACE) this percentage increased to 52% because the regional stratosphere was strongly affected by an active fire season. *INDEX TERMS:* 0305 Atmospheric Composition and Structure: Aerosols and particles (0345, 4801); 0322 Atmospheric Composition and Structure: Constituent sources and sinks; 0368 Atmospheric Composition and Structure: Troposphere—constituent transport and chemistry; *KEYWORDS:* biomass burning, single particle mass spectrometry, ITCT

Citation: Hudson, P. K., D. M. Murphy, D. J. Cziczo, D. S. Thomson, J. A. de Gouw, C. Warneke, J. Holloway, H.-J. Jost, and G. Hübler (2004), Biomass-burning particle measurements: Characteristic composition and chemical processing, *J. Geophys. Res.*, *109*, D23S27, doi:10.1029/2003JD004398.

1. Introduction

[2] Biomass-burning is a global phenomenon that results in large amounts of particles and trace gases being released into the atmosphere. The quantities and locations of particulates affect radiative balance and climate [*Fromm et al.*, 2000; *Fromm and Servranckx*, 2003; *Hobbs et al.*, 1997, 2003; *Kaufman and Fraser*, 1997; *Kirchstetter et al.*, 2003; *Mühle et al.*, 2002; *Sinha et al.*, 2003]. The composition of the particles plays a key role in understanding these issues. For example, composition affects their role as cloud condensation nuclei and the transport of elements into and out of burning regions [*Allen and Miguel*, 1995; *Andreae*, 1983; *Artaxo et al.*, 1994; *Echalar et al.*, 1995; *Gaudichet et al.*, 1995; *Kreidenweis et al.*, 2001; *Lelieveld et al.*, 2001; *Li et al.*, 2003; *Liu et al.*, 2000; *Pósfai et al.*, 2003].

[3] A fingerprint or signature of biomass-burning particle composition is difficult to obtain as the composition has been found to vary significantly with the biomass burned, the conditions of the burn (whether the fire is flaming or smoldering), and the surrounding atmospheric conditions [*Echalar et al.*, 1995; *Gao et al.*, 2003; *Hays et al.*, 2002; *Ikegami et al.*, 2001; *Sheesley et al.*, 2003; *Sinha et al.*, 2003]. Bulk filter measurements followed by techniques to determine ionic compositions have sampled particles from burning biomass in both the laboratory and field. Potassium is a common component to the particulate measurements [*Allen and Miguel*, 1995; *Andreae*, 1983; *Andreae et al.*, 1998; *Echalar et al.*, 1995; *Gao et al.*, 2003; *Gaudichet et al.*, 1995; *Hays et al.*, 2002; *Kreidenweis et al.*, 2001]. The source strength and variability of potassium as an absolute

[1]NOAA Aeronomy Lab, Boulder, Colorado, USA.
[2]Also at Cooperative Institute for Research in Environmental Sciences, University of Colorado, Boulder, Colorado, USA.
[3]Bay Area Environmental Research Institute, Sonoma, California, USA.

0148-0227/04/2003JD004398$09.00

marker, however, is questionable. Potassium levels vary with fuel type and burn conditions [*Hays et al.*, 2002; *Kreidenweis et al.*, 2001]. Ion concentrations are often higher in flaming rather than smoldering conditions [*Echalar et al.*, 1995]. Aged combustion material also tends to release lower particulate concentrations of the elements Ca, Mg, K, Cl and ionic species nitrate and ammonium compared to the combustion of live foliage [*Hays et al.*, 2002]. Furthermore, the emission of potassium from other sources must also be considered. For example, there is potassium in smoke from meat charbroiling, although significantly less than in biomass smoke [*Sheesley et al.*, 2003]. Aging or processing of smoke particles has been identified by the accumulation of sulfate and/or nitrate on particles collected downwind of sources [*Andreae et al.*, 1998; *Gao et al.*, 2003; *Gaudichet et al.*, 1995; *Kreidenweis et al.*, 2001; *Liu et al.*, 2000].

[4] Analyses of single particles collected on grids and later analyzed by transmission electron microscopy (TEM) with energy-dispersive X-ray spectrometry (EDS), and electron energy loss spectroscopy (EELS) also detect the presence of potassium [*Li et al.*, 2003; *Pósfai et al.*, 2003]. These single particle measurements also provide information about the internal and external mixing composition properties of particles. Most recent studies report organic particles with inorganic, potassium-rich, inclusions that are separate from soot particles [*Li et al.*, 2003; *Pósfai et al.*, 2003]. Bulk studies are unable to show this type of detail. Again, the aging of particles is inferred by the amassing of sulfate and nitrate [*Ikegami et al.*, 2001; *Li et al.*, 2003; *Pósfai et al.*, 2003]. Although TEM, EDS, and EELS provide more information about the biomass-burning particle composition than bulk measurements, such measurements are labor intensive, and volatile species are often lost from the collected particles [*Pósfai et al.*, 2003].

[5] Single particle mass spectrometers have the same benefits of the single particle techniques just mentioned and furthermore are able to make individual particle measurements with in situ analysis of the composition such that fewer volatile species are lost. Some drawbacks that single particle mass spectrometers have are the particle size and potential particle shape discrimination inherent in particle transmission to the instrument through the inlet. Prior to this current study, one other single particle mass spectrometer, the Aerosol Time-of-Flight Mass Spectrometer (ATOFMS), was used for both laboratory and field measurements yielding information on biomass-burning particle composition [*Guazzotti et al.*, 2001, 2003; *Silva et al.*, 1999]. For laboratory studies, a variety of biomass was burned within the lab and percent occurrences of various ions were reported. Potassium was the most common ion detected, present in greater than 90% of the samples obtained [*Silva et al.*, 1999]. The ATOFMS instrument, deployed during the Indian Ocean Experiment (INDOEX), correlated particle composition measurements to gas-phase measurements of acetonitrile [*Guazzotti et al.*, 2003], which has been shown to be a good biomass-burning tracer [*de Gouw et al.*, 2003b; *Holzinger et al.*, 1999; *Singh et al.*, 2003]. With this information, in combination with back trajectories, a distinction between particles from biomass/biofuel sources and vehicular emission or fossil fuel combustion sources was determined by the respective presence or absence of potassium in carbon based particles [*Guazzotti et al.*, 2003].

[6] In this study, the Particle Analysis by Laser Mass Spectrometry (PALMS) instrument was used to measure the composition of individual particles from a two hour old fire plume intercepted over southern Utah [*Warneke et al.*, 2002] during the Intercontinental Transport and Chemical Transformation (ITCT) mission in spring of 2002. It is difficult to make direct comparisons between the PALMS and ATOFMS instruments due to differences in the laser power and wavelength used for ablating and ionizing the particles, which cause large differences in the sensitivity to ions as well as the fragmentation of molecules [*Guazzotti et al.*, 2001]. The ATOFMS uses a frequency quadrupled Nd:YAG ($\lambda = 266$ nm), as compared to the PALMS excimer ($\lambda = 193$ nm), to desorb and ionize species from the individual particles. The PALMS instrument more tightly focuses this beam, delivering a higher power density to the individual particles, which leads to more fragmentation of the ions.

[7] The current study provides the first in situ single particle measurements of composition from a natural forest fire, and combines those measurements with other airborne measurements. Two different methods were used to identify particles from biomass-burning sources using either the entire mass spectrum or individual mass peaks from a mass spectrum. The particle results are compared to gas-phase measurements using emission tracers of biomass-burning such as acetonitrile (CH_3CN) [*de Gouw et al.*, 2003b; *Holzinger et al.*, 1999; *Singh et al.*, 2003] and carbon monoxide (CO). The analyses were extended to other missions (WB-57 Aerosol Mission (WAM), Atmospheric Chemistry of Combustion Emissions near the Tropopause (ACCENT), ACCENT 2000, and Cirrus Regional Study of Tropical Anvils and Cirrus Layers – Florida Area Cirrus Experiment (CRYSTAL-FACE)) where gas-phase measurements of biomass-burning tracers were not available. Processing, or aging, of the particles is also inferred from the presence of sulfate on the particles.

2. Instrumentation

[8] The purpose of the ITCT mission was to measure air masses entering the United States, targeting Asian influenced plumes. Data were also acquired on transit flights and over Californian urban areas. The NOAA WP-3D aircraft was equipped with a wide variety of in situ gas-phase and particle instruments [*Brock et al.*, 2004; *Nowak et al.*, 2004]. Discussion of the gas and particle phase instrumentation as well as specific transport events is given by *Brock et al.* [2004], *de Gouw et al.* [2003a], and *Nowak et al.* [2004]. The instruments used for this analysis are discussed briefly here. A proton transfer reaction mass spectrometer (PTR-MS) measured mixing ratios of a number of organic species including acetonitrile [*de Gouw et al.*, 2003a]. The integration time varied per mass (one to two s) and the duration of the measurement cycle varied per flight (nine to 15 s) [*de Gouw et al.*, 2003a]. CO mixing ratios were measured using an ultraviolet fluorescence spectrometer [*Holloway et al.*, 2000] on a one second timescale. Particle and number density were obtained by combining measurements from a LasAir 1001A optical particle counter (OPC)

and a white light optical particle counter [*Brock et al.*, 2000].

[9] Particle composition measurements were obtained by the PALMS instrument, a single particle time-of-flight mass spectrometer that acquires either a positive or negative mass spectrum for individual particles that are detected and ablated. The instrument has been described in detail previously [*Thomson et al.*, 2000]. Briefly, a particle that enters the instrument is detected by a continuous frequency-doubled Nd:YAG laser (λ = 532 nm) and is then immediately ablated and ionized by a pulsed excimer laser (λ = 193 nm). Mass spectra are acquired for approximately 90% of the particles that are detected by the Nd:YAG laser. The ions are detected using the time-of-flight mass spectrometer producing a mass spectrum (detector signal versus mass-to-charge ratio) per individual particle. During the ITCT mission, the instrument was mounted in a right wing pod of the WP-3D aircraft. Ambient air was brought to the instrument through the same shrouded inlet that was used when the instrument was housed in the nose of the WB-57F aircraft for the WAM, ACCENT, ACCENT 2000, and CRYSTAL-FACE field campaigns [*Thomson et al.*, 2000]. An aerodynamic lens focuses the aerosol to the ion source region allowing for enhanced particle sampling [*Schreiner et al.*, 1999]. The transmission efficiency of the aerodynamic lens is roughly constant for particles in the 0.2 to 1 μm diameter range [*Cziczo et al.*, 2004]. Although the instrument is capable of measuring particles as large as 5 μm, the transmission efficiency decreases significantly for larger particles. On average for the ITCT mission, PALMS sampled 60% of the total volume sampled by the particle instruments mentioned above. This average is slightly lower (40%) for particles sampled between 500 m and 3 km. The instrument operated fully automated while on the aircraft, acquiring either positive or negative mass spectra with brief periods of time for laser realignment. Only positive mass spectra were acquired during the forest fire plume interception, therefore, only positive mass spectra will be presented and discussed here.

3. Forest Fire Plume Interception

[10] The WP-3D aircraft intercepted a forest fire plume over southern Utah during the ITCT mission in spring of 2002. Back trajectories and chemical tracers show the fire plume to be approximately two hours from its source at the point it was intercepted [*Warneke et al.*, 2002]. Figure 1 shows acetonitrile (CH_3CN), CO, and particle number measurements acquired during the plume crossing as a function of time. The acetonitrile mixing ratio increased from 200 to 1600 pptv [*de Gouw et al.*, 2003a]. Increases in particle number and CO also denote plume events from pollution or biomass-burning sources [*Brock et al.*, 2004]. Clear enhancements, highly correlated in fine structure, of each of these species over the background levels were observed on 20 May 2002 from 00:18:50–00:20:40 UTC. CO mixing ratios increased from 100 to nearly 900 ppbv. The number concentration of particles, corresponding to those that the PALMS instrument theoretically measures, increased by more than an order of magnitude. The geometric mean diameter of the biomass-burning particles sampled during this time period (not shown) is 0.28 μm with a geometric standard deviation of 1.43. The mean diameter slightly increased to 0.33 μm in the middle of the plume sampling.

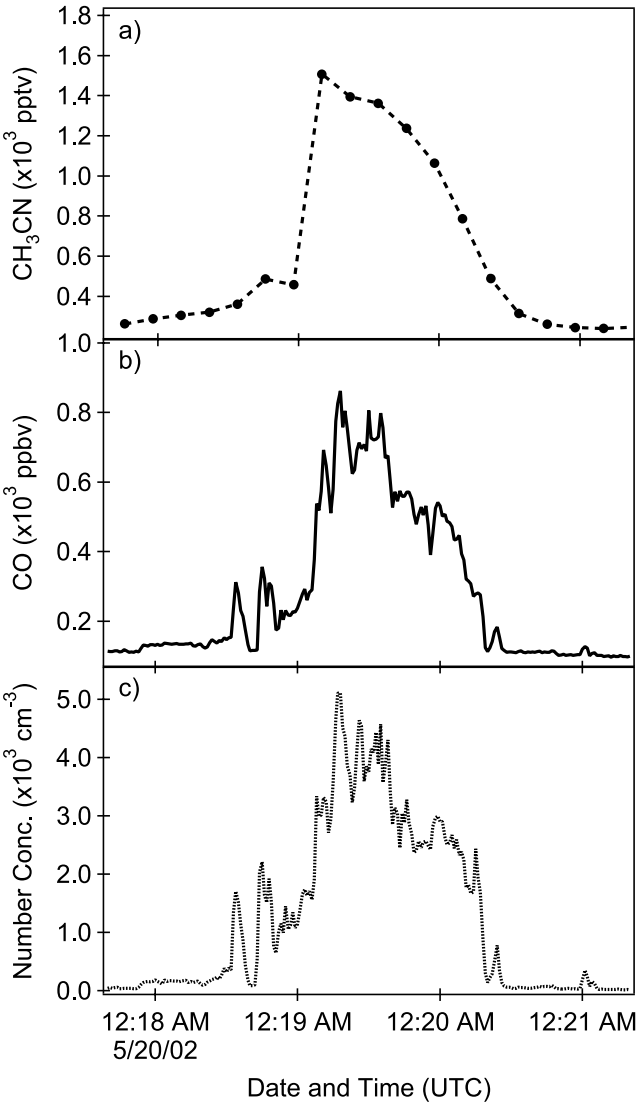

Figure 1. Time traces of gas-phase species (a) acetonitrile (CH_3CN) (pptv), (b) carbon monoxide (CO) (ppbv) and (c) number concentration (cm^{-3}) during forest fire plume transect on 19 May 2002.

[11] The PALMS instrument acquired 202 individual particle mass spectra during the 100 s plume crossing. A positive mass spectrum of a particle sampled during the plume crossing is shown in Figure 2. The particle contains carbon (m/z = 12, C^+), potassium (m/z = 39, K^+), a variety of organics at m/z = 24–29 (enhanced region shown in inset in Figure 2), and nitrogen containing compounds (m/z = 30, NO^+). The NO^+ peak may be due to either ammonium or nitrate in the particle. It is difficult to determine the source of the NO^+ without larger ion fragments present. However, previous studies, using different analytical methods, have indicated the presence of ammonium on fresh plume particles [*Andreae et al.*, 1998; *Hays et al.*, 2002; *Pósfai et al.*, 2003].

[12] The particles sampled during the plume crossing are consistent with previous reports of biomass-burning par-

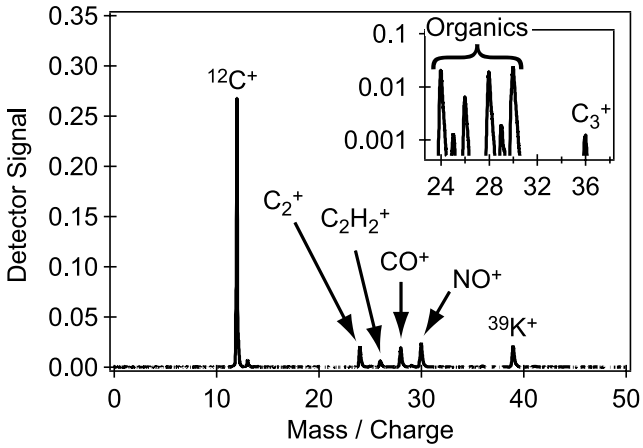

Figure 2. Mass spectrum of a particle acquired within the forest fire plume on 19 May 2002. Carbon, potassium, and organic ions are present. The inset in Figure 2a is an expansion of the spectrum between m/z = 24–38, using a log scale of the *y axis*, showing organic peaks as well as the C_3^+ (m/z = 36) peak that indicates the presence of soot within the particle.

ticles. In qualitative terms, these particles were organic particles with potassium, not pure soot particles [*Guazzotti et al.*, 2003; *Li et al.*, 2003; *Silva et al.*, 1999]. Although no pure soot particles were detected in this plume event, internally mixed soot may have contributed to the particle mass. A carbon soot pattern (C^+, C_2^+, C_3^+) may lie under the $^{12}C^+$ peak, and smaller C_2^+ (m/z = 24) peak that are from both organics and soot. A C_3^+ (m/z = 36) peak is shown in the inset of Figure 2.

[13] The presence of specific ions in the mass spectra acquired from the plume particles can be compared to results from the ATOFMS. As was mentioned previously, more than 90% of the particles sampled with ATOFMS from the combustion of biomass in the laboratory had an occurrence of potassium [*Silva et al.*, 1999]. This result is in good agreement with the PALMS particle composition from the forest fire plume where over 90% of the particles sampled within the plume contained potassium.

[14] Sodium was another common component to the ATOFMS biomass-burning particle composition, occurring in 15–70% of the combusted biomass particles and varying with biomass type [*Silva et al.*, 1999]. In contrast, no particles sampled within the fire plume during ITCT contained sodium. The lack of sodium in the Utah fire plume could be due to sensitivity differences between the ATOFMS and PALMS instruments. However, 20% of the biomass-burning particles sampled over the Los Angeles area during ITCT, a region similar to the *Silva et al.* [1999] measurements, contained sodium. This would point to a variable sodium content depending on the biomass material combusted, as was observed by *Silva et al.* [1999].

4. Biomass-Burning Particle Classification

[15] Two analysis techniques, discussed in detail in section 4.1 and 4.2, were applied to the mass spectra acquired during the plume crossing to develop objective tools for identifying the presence of biomass-burning particles in other data sets. One of these techniques, cluster analysis, proved to be a very stringent classification scheme that identified only freshly emitted biomass-burning particles similar in composition to those sampled during the fire plume interception. The second technique used individual mass peaks to produce a biomass-burning index. This biomass-burning index accounted for a majority of the local events but also identified long-range transport events and biomass-burning particles that had been chemically processed, as inferred from the addition of sulfate and nitrate. The combination of these two methods allowed for identification of local versus transported sources of biomass-burning particles.

4.1. Cluster Analysis

[16] The mass spectra of the particles sampled within the fire plume were similar from particle to particle. A clustering algorithm based on the presence and relative areas of all peaks within a spectrum has been used to categorize mass spectra from an entire mission into smaller groupings to facilitate data analysis [*Murphy et al.*, 2003]. This algorithm was applied to the 202 particle mass spectra acquired during the plume crossing. The largest of the resulting categories from the clustering algorithm accounted for 122 of the 202 particles. A representative mass spectrum from this category is shown in Figure 2.

[17] To search for spectra similar to the majority of spectra acquired during the plume crossing, an arithmetically averaged mass spectrum was produced from combining the 122 mass spectra of the top category after each spectrum was normalized. This averaged mass spectrum was used as the representative biomass-burning particle to which all other particle mass spectra were compared. If a particle mass spectrum was greater than 90% correlated to the averaged mass spectrum, it was identified as a biomass-burning particle. A small number (9 of 122) of particles originally placed within the largest category were not greater than 90% correlated to the averaged mass spectrum. This is to be expected, as the requirements for the original clustering are looser than the 90% correlation threshold employed for this particular analysis. Additionally, 13 mass spectra that had been placed in the second largest cluster were correlated at >90% to the vector of the averaged mass spectrum from the top category. In total, 126 of the 202 particles (62%) sampled within the fire plume were identified as biomass-burning particles by the cluster analysis method. For example, the mass spectrum shown in Figure 2 is correlated >95% with the averaged mass spectrum in the top cluster.

[18] Figure 3 shows the fraction of particles identified as biomass-burning particles according to the two analysis methods for a number of events that will be discussed throughout the paper. The 62% of particles identified by the cluster analysis from the Utah fire plume is shown in Figure 3 as ITCT plume.

4.2. Biomass-Burning Index

[19] A majority of the particle mass spectra acquired during the plume crossing were similar to that shown in Figure 2. The remainder of the particles sampled during the plume crossing contained the same potassium, carbon, and

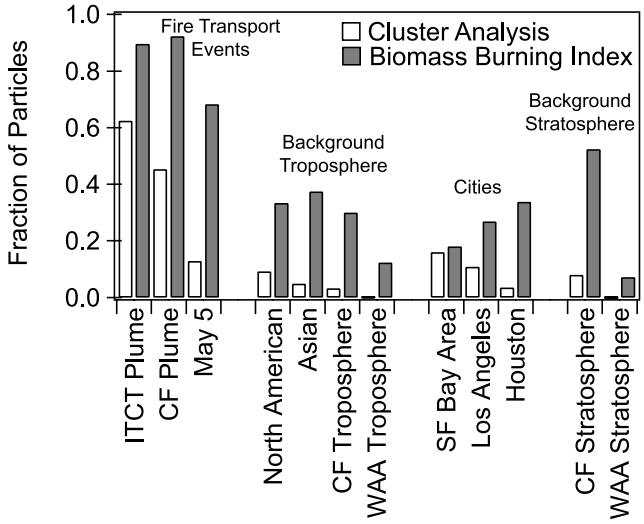

Figure 3. Percentage of particles attributed to biomass-burning according to the two analysis methods, cluster analysis (open bars) and biomass-burning index (solid bars), for fresh (ITCT plume and CRYSTAL-FACE (CF) plume) and aged (5 May) fire event, North American and Asian backgrounds and cities (obtained during ITCT), and tropospheric and stratospheric backgrounds for the CF and WAM, ACCENT, and ACCENT 2000 (WAA) missions.

organics but often a much larger potassium peak relative to the carbon peak was observed. Furthermore, the ratio of the larger potassium peak to the carbon peak was not as consistent as in the mass spectra from the largest cluster.

[20] Because of the known variability in the mass spectra of biomass-burning particles, the second analysis method used individual peak areas from a mass spectrum, specifically the presence of both carbon and potassium, to identify biomass-burning particles. In previous studies, potassium has been used as a chemical component in identifying biomass-burning particles [*Allen and Miguel*, 1995; *Andreae*, 1983; *Andreae et al.*, 1998; *Echalar et al.*, 1995; *Gao et al.*, 2003; *Gaudichet et al.*, 1995; *Hays et al.*, 2002; *Kreidenweis et al.*, 2001]. A qualitative signature developed by *Kreidenweis et al.* [2001] uses the ionic composition of bulk particle measurements obtained from the IMPROVE network that are analyzed by particle induced x-ray emission (PIXE) and x-ray fluorescence (XRF) techniques. Smoke is identified from a qualitative signature for non-soil potassium (KNON), calculated by subtracting 60% of the iron (Fe) quantity from the potassium signal to correct for potassium from crustal sources [*Kreidenweis et al.*, 2001].

[21] The identification scheme for the biomass-burning index applied this same type of rationale to an individual mass spectrum. Previous studies have shown that potassium is a consistent marker in biomass-burning particles. However, it is also a common component in sea salt, minerals, meteoritic material, and particles from industrial sources. These particles also contain elements not observed in the biomass-burning particles sampled in the fire plume crossing such as aluminum (m/z = 27), iron (m/z = 56), and lead (m/z = 208). As a result, empirical ratios of a number of elements were subtracted from the potassium signal for each individual particle such that for particles containing potassium from sea salt, minerals, meteoritic material and industrial sources the modified potassium signal becomes negative. The ratios used in the calculation of the biomass-burning index are based on examination of the potassium signal in a plethora of spectra from identifiable sources. On a particle-to-particle basis, the potassium area was empirically corrected according to equation (1):

$$MA_{39} = A_{39} - (4A_{23} + A_{27} + 5A_{40} + 10A_{51} + 4A_{56} + 10A_{120} + 20A_{208}) \quad (1)$$

Here, $A_{\#}$, where # = 39, 23, 27, etc., is the relative area under the peak at m/z = # in an individual particle mass spectrum. The species used to modify the potassium signal are present in mass spectra from sea salt (m/z = 23, Na^+), minerals or meteoritic material (m/z = 27, Al^+; m/z = 40, Ca^+; m/z = 56, Fe^+), and industrial sources (m/z = 51, V^+; m/z = 120, Sn^+; m/z = 208, Pb^+). The multiplicative factors were determined empirically to create negative MA_{39} values for particles clearly identified as sea salt, minerals, meteoritic material, and from industrial sources. Negative values of MA_{39} were set to zero thus removing these particles from the analysis. For example, in a typical sea salt spectrum, $A_{23} = 0.77$ and $A_{39} = 0.08$. Therefore the value of $MA_{39} = -3$ would be set to zero. These empirical factors used were generous to allow for particle-to-particle variability in ionization.

[22] This modified potassium peak was then combined with the carbon peak (m/z = 12) to yield a value that was related to the amount of carbon and potassium within a particle mass spectrum by equation (2):

$$\textit{Biomass-burning index} = \frac{\left[(A_{12})(MA_{39})^2\right]^{1/3}}{0.529} \quad (2)$$

The product of the relative areas of A_{12}, carbon, and MA_{39}, modified potassium, was used rather than an additive combination to make the biomass-burning index, defined in equation (2), zero if either peak was not present. The index is weighted toward m/z = 39 being a more unique indicator of biomass-burning than m/z = 12, carbon, and potassium is therefore factored into the equation twice. The quantity is raised to the power of 1/3 for the purposes of keeping constant units. If the carbon and potassium peaks were the only peaks present, the factor of 0.529 normalizes the possible values of the biomass-burning index from 0 to 1.0. The index was further modified to exclude particles with large m/z = 24 peaks that could be due to magnesium (Mg^+). If m/z = 24 were only from carbon, the ratio of m/z = 12 to m/z = 24 was normally greater than two. Therefore if this ratio was less than two, the biomass-burning index was set to zero.

[23] The median m/z = 12 (C^+) and m/z = 39 (K^+) relative peak areas in biomass-burning particles are 0.34 and 0.22 yielding a biomass-burning index of 0.48. Although the index was designed to range from zero to one, it was unclear that an index of 0.9 represented "more" biomass-burning characteristics than that of 0.1. As a result, a threshold of a biomass-burning index greater than 0.05 was used to designate biomass-burning particles. If only carbon and

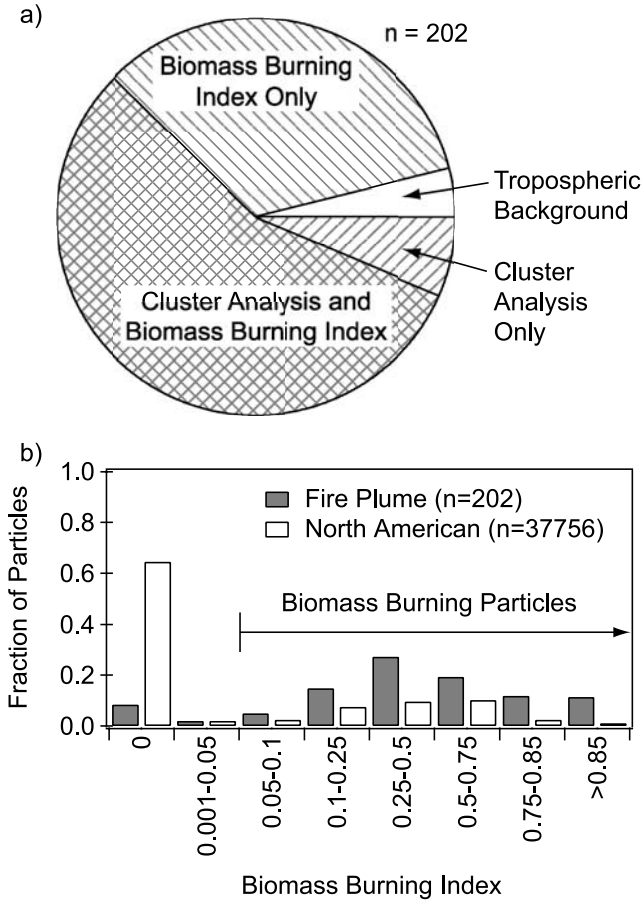

Figure 4. Figure 4a shows the distribution of the 202 particles sampled from the Utah fire plume by their analysis methods for identified biomass-burning particles. 56% of the particles were identified by both the cluster analysis and the biomass-burning index (crosses). 6% were identified by only the cluster analysis (up slash). 34% were identified by only the biomass-burning index (down slash). 4% were typical of background tropospheric particles (open). Figure 4b shows the biomass-burning index value of fire plume particles and North American background particles. The biomass-burning index threshold of 0.05 identified the majority of fire plume particles. 65% of the particles in the North American background have a biomass-burning index of zero, which identified particles with no potassium.

potassium were present in the particle, the threshold of 0.05 allowed for a relative potassium area to be as small as 0.5% (0.005) of the total ion current or as large as 99% (0.99) of the total ion current to be identified as a biomass-burning particle. The smallest and largest potassium fractions observed for biomass-burning particles during the plume crossing were 0.1 and 0.9 respectively where carbon and potassium were typically 80% of the total ion current. Because the biomass-burning index was able to accommodate the wide range of potassium to carbon relative peak areas present in some of the particle mass spectra acquired during the plume crossing, 90% of the particles sampled within the plume were identified as biomass-burning particles, compared to the 62% identified by the cluster analysis (Figure 3, biomass-burning index, ITCT plume).

[24] In both characterization techniques, the numerical constraints for the correlation in the cluster analysis and the biomass-burning index were purely empirical. Because the observed plume was aged ~2 hours in the troposphere [*Warneke et al.*, 2002], it was not expected that all particles be identified as biomass-burning particles. The values (>0.9 for cluster analysis and >0.05 for biomass-burning index) were chosen with respect to particles sampled within the fire plume. The distribution of plume particles identified by the cluster analysis, biomass-burning index or both techniques is shown in Figure 4a. 56% of the 202 particles were identified by both analysis methods. An additional 6% were identified by only the cluster analysis. An additional 34% were identified by only the biomass-burning index. 4% were representative of background tropospheric particles. Figure 4b shows the distribution of the biomass-burning index for all particles sampled within the fire plume. For comparison, the distribution of the biomass-burning index for particles sampled from the North American background (boundary defined in section 5.2) are also shown. Only a small fraction of particles in the fire plume (10%) had a biomass-burning index less than 0.05. Close to half of those particles were identified by the cluster analysis but the absence of potassium prevented them from being identified by the biomass-burning index. In contrast, the North American background had a large fraction of particles (65%) with a biomass-burning index equal to zero and only 5% of those particles were identified by the cluster analysis. The biomass-burning particles (biomass-burning index >0.05) in the North American background also have a similar distribution of biomass-burning indices as the Utah fire plume.

5. Lower and Middle Tropospheric Measurements

5.1. Identification of Transport Events

[25] Two transport events, identified by the particle analyses and supported by gas-phase measurements and modeled results, are discussed in this section. On 22 April 2002, during the transit from Tampa, FL to Monterey, CA, a fire plume was intercepted east of Houston from a fire in the Yucatan Peninsula [*Warneke et al.*, 2002]. On 5 May 2002, off the west coast of California, a plume attributed to biomass combustion was intercepted at altitudes greater than 7 km that was transported from Asia [*Brock et al.*, 2004; *Cooper et al.*, 2004; *de Gouw et al.*, 2004; *Nowak et al.*, 2004; *Warneke et al.*, 2002]. For the 22 April 2002 plume interception acetonitrile levels increased from a background of 150 pptv to 600 pptv. CO levels increased from 100 ppbv to nearly 300 ppbv. Unfortunately, there was approximately a five minute gap in the PALMS positive data at the time of the maximum CO and acetonitrile levels when negative spectra were acquired followed by a laser alignment. However, the percentage of biomass-burning particles identified increased just prior to and decreased after the event.

[26] On the 5 May 2002 transport event large enhancements in acetonitrile (600 pptv), CO (200 ppbv), and fraction of biomass-burning particles were observed relative to background levels [*Brock et al.*, 2004; *de Gouw et al.*, 2004]. The transport time of the 5 May event was approximately eight days. Figure 3 shows the relative fraction of

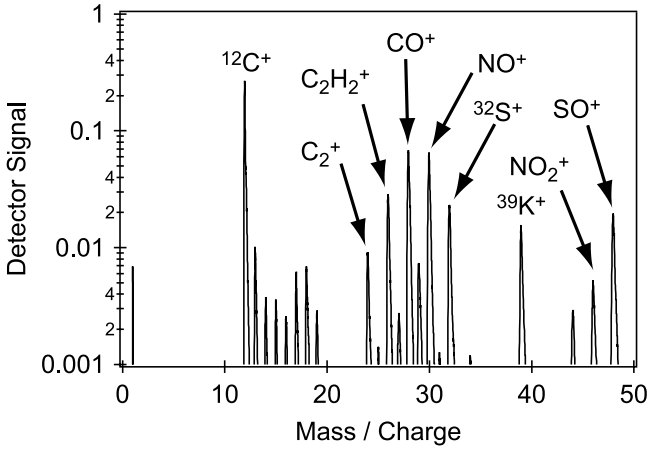

Figure 5. Mass spectrum of a particle sampled during the May 5 transport event identified by the biomass-burning index. The detector signal is on a log scale for ease in identifying small peaks. Note the addition of sulfate (m/z = 32, S^+; m/z = 48, SO^+) and nitrate (m/z = 46, NO_2^+) to this transported particle relative to non-aged particle shown in Figure 2.

biomass-burning particles for the 5 May transport event by the cluster analysis and the biomass-burning index. Most likely due to mixing in of other particles, the identified biomass-burning particle fraction for the 5 May event with respect to both analysis methods was smaller relative to the Utah fire plume (ITCT plume). The 5 May event had 13% biomass-burning particles defined by the cluster analysis and 68% defined by the biomass-burning index. This may be compared to 62 and 90% respectively for the fire plume.

[27] Figure 5 shows a mass spectrum for a particle sampled during the 5 May transport event. The detector signal is plotted on a log scale to enhance the ability to see small peaks. This spectrum was not identified by the cluster analysis, due to additional peaks in the mass spectrum from sulfate ($^{32}S^+$; m/z = 48, SO^+) and nitrate (m/z = 46, NO_2^+), species not present in the fresh plume particle (see Figure 2). The biomass-burning index was greater than 0.05 and therefore identified it as a biomass-burning particle because it contained carbon and potassium that was not associated with ions typical of mineral or sea salt particles.

5.2. Biomass-Burning Particles Outside Known Transport Events

[28] The transport events of 22 April and 5 May are known biomass-burning events based on simultaneous acetonitrile measurements. Biomass-burning particles were also observed in other regions even though gas-phase tracers such as acetonitrile were not above background levels. Figure 3 shows the fraction of particles identified as biomass-burning particles for a North American background, Asian background, and specific urban areas that were sampled during the ITCT mission (Houston, Los Angeles, and the San Francisco Bay area). The sampling areas determined to have been impacted by Asian plumes are described in detail in *Brock et al.* [2004] and *Nowak et al.* [2004]. Briefly, they contained particles above the boundary layer that were not influenced by North American sources and were transported over the Pacific Ocean to the US west coast. The North American background excluded Asian transport, the urban regions described below, and the forest fire interception over Utah. The three urban regions were defined in latitude/longitude space: Houston latitude 29.2° to 30.2° and longitude −95.9° to −94.7°; Los Angeles latitude 33° to 35° and longitude −119.1° to −116.1°; San Francisco Bay area latitude 36° to 38.75° and longitude −123.4° to −121.4°.

[29] As shown in Figure 3, the fraction of particles identified by the cluster analysis and biomass-burning index for the North American background are 9% and 33% respectively. For the Asian transport, the fraction of particles identified by the cluster analysis decreases to 5% and the fraction of particles identified by the biomass-burning index increases to 37%. It would be expected that the majority of plume events from Asia would be processed during transport while it is still possible to intercept fresh plumes in the North American background supporting the result of the cluster analysis identifying fresh biomass-burning particles and the biomass-burning index identifying those that have been chemically processed.

[30] The fraction of particles identified by the biomass-burning index in the urban areas are comparable to that of the North American background with the highest fraction in Houston decreasing to the Los Angeles and San Francisco Bay areas. The opposite trend is observed in the fraction of particles identified by the cluster analysis with the fraction of particles increasing from Houston to Los Angeles and the San Francisco Bay area. The distribution of particles between the cluster analysis and biomass-burning index was further examined using MODIS fire information for 2002 (available at http://firemapper.sc.egov.usda.gov/modispts/modisfire_2002.htm). No local fires were present in the Houston area and therefore a small percentage of biomass-burning particles were identified by the cluster analysis. A larger percentage of biomass-burning particles were identified by the biomass-burning index relative to the other urban areas. The defined region for the Houston area does overlap the region of the interception of the Yucatan Peninsula plume and was likely to be influenced by that transported plume. Local fires were present in both the San Francisco Bay and Los Angeles areas prior to transit through these regions that could account for the larger fraction of particles identified by the cluster analysis relative to Houston. Although these observations do provide support for the analysis methods identifying either fresh or processed biomass-burning particles, a "clean" urban signature, not influenced by biomass-burning, was not observed during the ITCT mission.

[31] Although the urban areas and the North American background have a similar fraction of particles identified as having a biomass-burning origin, the number density of particles within the urban areas was much larger than in the general background. This translates to an overall higher number of biomass-burning particles. However, no strong correlation existed between power plant or gas-phase urban signatures and the presence of biomass-burning particles.

The possibility that the cluster analysis and biomass-burning index identified biomass production from wood burning stoves or meat cooking facilities still exists and cannot be discerned without further measurements.

6. Upper Tropospheric/Lower Stratospheric Measurements

6.1. CRYSTAL-FACE Biomass-Burning Plume

[32] In July 2002, the PALMS instrument was flown on the NASA WB-57F aircraft during the Cirrus Regional Study of Tropical Anvils and Cirrus Layers - Florida Area Cirrus Experiment (CRYSTAL-FACE) mission. Figure 6a shows two minute time averages of the fraction of particles attributed to biomass-burning by the cluster analysis and the biomass-burning index when positive mass spectra were acquired. High particle fractions were observed on 9 July 2002 between 19:36:50 and 20:00:00 UTC around 15 km altitude. Figure 6b shows simultaneous gas-phase measurements of CO and ozone (O_3) on 9 July. CO was measured using the NASA Ames ARGUS instrument, a tunable diode laser configured to measure CO in the mid-infrared [*Loewenstein et al.*, 2002]. O_3 was measured using the NOAA O_3 instrument [*Proffitt and McLaughlin*, 1983]. Using O_3 as an altitude measure, this particle-identified biomass-burning plume shows a large enhancement in CO (mixing ratios up to 160 ppbv) over the typical stratospheric background with mixing ratios of 30–50 ppbv. A paper combining the in situ measurements made during the CRYSTAL-FACE mission with remote sensing and modeling discusses the plume event on 9 July in detail [*Jost et al.*, 2004]. Back trajectories trace this plume to boreal forest fires in Canada approximately 13 days prior to 9 July [*Jost et al.*, 2004]. The mass spectra of particles sampled during this interception are indistinguishable from those measured during the fire plume interception over Utah on 19 May 2002. Shown in Figure 3, the biomass-burning index analysis identified 92% of the particles within this ~24 min interval as biomass-burning particles. More interestingly, the cluster analysis also identified 45% as biomass-burning particles, indicating little chemical change to the particles had taken place since emission despite the 2 week transport time.

[33] Observations of the transport of forest fire smoke into the stratosphere have also been previously reported using remote sensing techniques [*Fromm et al.*, 2000; *Fromm and Servranckx*, 2003]. In situ measurements of trace gases typical for biomass-burning were intercepted at ~10 km altitude from 10°S to 10°N during the Civil Aircraft for the Regular Investigation of the atmosphere Based on an Instrumented Container (CARIBIC) flight from Namibia to Germany, due to deep convection [*Mühle et al.*, 2002].

6.2. Background Measurements

[34] Outside of this stratospheric plume, other WB-57F measurements in the upper troposphere and lower stratosphere were analyzed for biomass-burning particles. For the purposes of this discussion, the stratosphere and troposphere were identified using O_3 measurements also on the WB-57F. The stratosphere was defined with an O_3 lower limit of 200 ppbv and the troposphere with an O_3 upper limit of 100 ppbv; measurements made when O_3 was between 100 and 200 ppbv were not considered. The fraction of biomass-burning particles is reported for the CRYSTAL-FACE troposphere (CF troposphere) and CRYSTAL-FACE stratosphere (CF stratosphere) in Figure 3. The CF tropospheric measurement is very similar to that of the ITCT North American percentage as identified by the biomass-burning index (~30%). Approximately 50% of the particles sampled in the stratosphere during the CRYSTAL-FACE mission were identified by the biomass-burning index. This is ascribed to the active fire season during the CRYSTAL-FACE mission. The outflow from large fires in Canada and Colorado was injected into the stratosphere and transported to the sampling region during CRYSTAL-FACE. As a result, abnormally high levels of biomass-burning

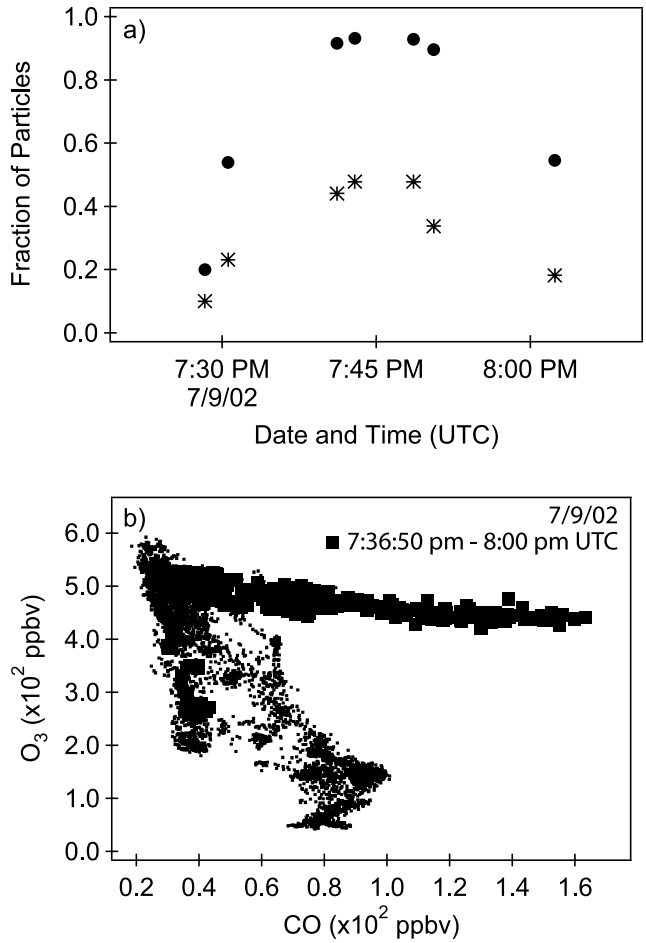

Figure 6. Figure 6a shows a two minute time average of fraction of particles identified by both the biomass-burning index (closed circles) and cluster analysis (asterisks) before and after the period of the plume interception in the stratosphere, ~15 km altitude, on 9 July 2002 during the CRYSTAL-FACE (CF) mission. Figure 6b shows an O_3 versus CO plot of all data obtained on 9 July in dots and for the time period of the plume interception in solid squares. Anomalously high levels of CO were observed at high O_3 levels (high altitudes).

particle fractions were sampled regionally in the lower stratosphere for the CRYSTAL-FACE measurement period.

[35] In 1998, 1999, and 2000, the PALMS instrument was also flown on the WB-57F during the WAM, ACCENT, and ACCENT 2000 missions (WAA), respectively, that surveyed a wide range of latitudes in the eastern and central United States. A key instrumentation difference between the 2002 missions and those prior was a capillary inlet used during the WAA missions that biased particle measurements to larger particle sizes [*Cziczo et al.*, 2003; *Middlebrook et al.*, 2003]. Because the biomass-burning particles are mostly sub-micron, they would not have been sampled as efficiently prior to 2002.

[36] Figure 3 shows the fraction of biomass-burning particles identified by the cluster analysis and biomass-burning index for the WAA missions in the troposphere and stratosphere. Essentially no particles were identified by the cluster analysis during the WAA missions in either atmospheric region. Much smaller fractions of biomass-burning particles were identified by the biomass-burning index in the troposphere during WAA, relative to the other tropospheric measurements, most likely due to the inlet differences. However, with respect to the stratosphere, as the only comparison is relative to a known enhanced fire season (CF stratosphere, 52%), the 7% could be a reasonable percentage but is likely slightly low, again, due to inlet differences.

7. Sulfate as an Indicator of Aging

[37] Increases in sulfate and nitrate within aging plumes have been commonly observed by a number of techniques [*Andreae et al.*, 1998; *Gao et al.*, 2003; *Gaudichet et al.*, 1995; *Ikegami et al.*, 2001; *Kreidenweis et al.*, 2001; *Li et al.*, 2003; *Liu et al.*, 2000; *Pósfai et al.*, 2003]. The amount of gas-phase SO_2 released from a fire plume of different biomass or the oxidizing capability of the atmosphere may affect the amount of sulfate observed on aging particles [*Ikegami et al.*, 2001; *Kreidenweis et al.*, 2001; *Li et al.*, 2003; *Pósfai et al.*, 2003]. Regional enhancements of sulfate content have also been reported previously [*Ikegami et al.*, 2001; *Kreidenweis et al.*, 2001].

[38] Figure 5 shows a mass spectrum for a particle sampled during the May 5 transport event. All of the elements observed in the fresh particle mass spectra (Figure 2) are present including carbon (m/z = 12), potassium (m/z = 39), organics (m/z = 24–29) and the NO^+ peak at m/z = 30. Here, the additional peak at m/z = 46 (NO_2^+) infers the addition of nitrate to the particle. The addition of sulfate to the particle can be seen at m/z = 32 and 48 (S^+ and SO^+ respectively). The presence of sulfate and nitrate on biomass-burning particles identified by the biomass-burning index can be used with additional knowledge of other trace gases and back trajectories to examine the presence of sulfate and nitrate as indicators of aged particles. However, nitrate is a much more complex species to understand in the atmosphere and the observation in mass spectra is not completely understood. Therefore only sulfate as an indicator of aging is discussed and only the sulfate on particles identified via the biomass-burning index is discussed because the cluster analysis identified particles have no sulfate as defined by the analysis. Figure 7 shows a summary of the median relative peak area of sulfate (m/z = 48, SO^+) on particles in each of the regions discussed previously. The vertical bars denote the quartiles. It is reasonable to compare sulfate content on particles identified by the biomass-burning index because the biomass-burning particles are very similar chemically and in turn the particle matrices are similar.

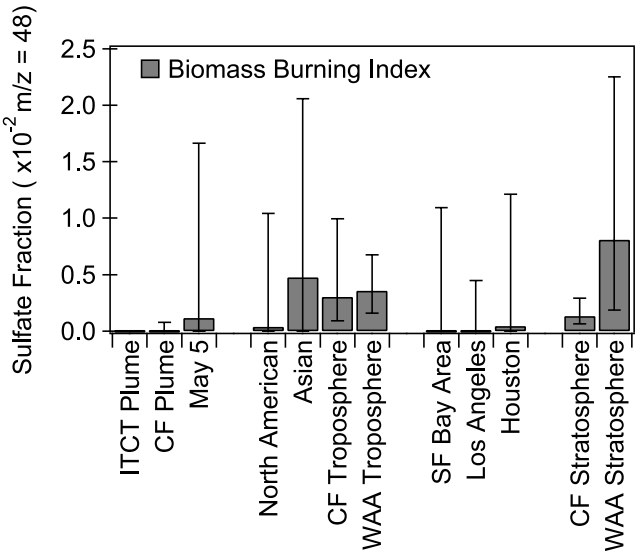

Figure 7. Median sulfate (m/z = 48, SO^+) fraction on particles identified by the biomass-burning index for all events in Figure 3. The vertical bars denote the 75 and 25 percentile values. Fresh plume events have lower median sulfate peak areas than aged events. Sulfate levels for tropospheric and stratospheric backgrounds are typically higher than all events with the exception of the North American and the CRYSTAL-FACE (CF) background due to their relatively fresh biomass-burning particles. The CF plume is a notable exception that was rapidly injected into the stratosphere and was likely not as processed as the other background stratospheric measurements.

[39] Fresh events have lower median sulfate peak areas than aged or transported events. For example, the ITCT fire plume, the San Francisco Bay and Los Angeles areas affected by local fires, and the North American background of local, lower tropospheric air masses, have much smaller median peak areas for sulfate than the 5 May transport event, the Asian influenced transport, the Houston area (which was affected by the long-range transport of a fire from the Yucatan Peninsula) or either of the upper tropospheric backgrounds for CRYSTAL-FACE or WAA. The stratospheric measurements, including the CRYSTAL-FACE plume, are not as straightforward. Although the CRYSTAL-FACE plume was intercepted well into the stratosphere, ~15 km altitude, it had essentially no sulfate present as compared to the CRYSTAL-FACE and WAA stratospheric backgrounds. Particles injected directly into the stratosphere, with little SO_2 present, may undergo little processing, and in turn would have small sulfate peaks. The CRYSTAL-FACE plume was quite dense (>90% biomass-burning particles) so any sulfate would be distributed among many particles. Additionally, little mixing of outside

particles within the plume (as observed by the high percentages of biomass-burning particles identified by either method in Figure 3) did not allow for much processing of the particles. The particles outside of the CRYSTAL-FACE plume had more mixing with other particles and the percentage of biomass-burning particles decreased and the median sulfate peak area increased. The particles intercepted during WAA may have been transported more slowly to the stratosphere allowing for more sulfate processing to take place.

[40] The PALMS sulfate is not directly comparable to that of other methods. For example, some cases report the presence of sulfate adsorbed on particles within 15 min of a fire plume [*Li et al.*, 2003]. The particles from the 2-hour aged fire plume of 19 May had no indication of sulfate. Because PALMS is not as sensitive to sulfate in the positive ion spectra as in the negative ion spectra, the use of m/z = 48 (SO^+) may not be a comparable sulfate marker compared to that used by *Li et al.* [2003]. Furthermore, it is used here as an indicator of chemically processed aging rather than chronological aging. For example, the CRYSTAL-FACE plume had been transported for approximately 13 days but showed little sign of chemical processing as indicated by the absence of sulfate.

8. Conclusions

[41] The PALMS instrument acquired single particle positive mass spectra from biomass-burning particles when the WP-3D aircraft intercepted a forest fire plume over southern Utah during the ITCT-2K2 field mission in spring of 2002. Fresh fire plume particles contain carbon, organics, potassium and ammonium ions. The particles are shown to incorporate sulfate with aging during transport if sulfur sources are present. In general, the presence of sulfate on biomass-burning particles is a good identifier of chemically processed events typically associated with long-range transport events. However, as seen in the case of the CRYSTAL-FACE plume, long-range transport events may not have been chemically aged.

[42] Biomass-burning particles from local and long-range transport events were identified by two analysis techniques presented in this study. The cluster analysis was based on mass spectra similar to those acquired from a fire plume aged two hours. In turn, it should only identify particles resembling those recently emitted from burning sources from a similar biota that did not undergo significant chemical transformation during transport. Interestingly, the cluster analysis was able to identify large percentages of biomass-burning particles across the United States in addition to a large plume intercepted at 15 km altitude, all events from presumably different biomass sources. The empirical biomass-burning index identified biomass-burning particles regardless of the addition of secondary inorganic material such as sulfate and nitrogen compounds. Gas-phase measurements of biomass-burning trace species support these identifications for both local and aged plumes. Discrepancies in potassium and sodium occurrence in particles are found in comparison to measurements reported from the Aerosol Time-of-Flight Mass Spectrometer (ATOFMS). However these differences can be explained by the variability of potassium and sodium emissions with fuel type and burn conditions as well as variability in instrument sensitivity to ions.

[43] A number of plume events were correctly identified from combustion of a wide variety of biomass. The biomass-burning index was capable of identifying combustion particles within a Utah forest fire plume, a plume from the Yucatan Peninsula, biomass-burning layers transported from Asia, and a boreal forest fire from Canada in the stratosphere. The percentages of biomass-burning particles in background tropospheric and stratospheric air masses have been examined over four years of observations. The percentages reported are biased due to the size range of the particles measured by PALMS and by the sampling regions of the aircraft. These errors are believed to be larger than the errors from the statistics associated with the reported percentages. Approximately 30% of the particles sampled in the lower troposphere were identified as biomass-burning particles. During the WAM, ACCENT, and ACCENT 2000 mission, ~7% of particles sampled in the lower stratosphere over the central and eastern United States were identified as biomass-burning particles. A large biomass-burning plume event was present during the CRYSTAL-FACE mission and as a result 52% of the particles sampled in the regional stratosphere were identified as originating from biomass-burning sources.

[44] **Acknowledgment.** The authors would like to thank Chuck Brock, Max Loewenstein, David Parrish, Erik Richard, and Fred Fehsenfeld for their insightful comments and helpful discussions.

References

Allen, A. G., and A. H. Miguel (1995), Biomass-burning in the Amazon: Characterization of the ionic component of aerosols generated from flaming and smouldering rainforest and Savannah, *Environ. Sci. Technol.*, *29*(2), 486–493.

Andreae, M. O. (1983), Soot carbon and excess fine potassium: Long-range transport of combustion-derived aerosols, *Science*, *220*(4602), 1148–1151.

Andreae, M. O., et al. (1998), Airborne studies of aerosol emissions from savanna fires in southern Africa: 2. Aerosol chemical composition, *J. Geophys. Res.*, *103*(D24), 32,119–32,128.

Artaxo, P., F. Gerab, M. A. Yamasoe, and J. V. Martins (1994), Fine mode aerosol composition at three long-term atmospheric monitoring sites in the Amazon Basin, *J. Geophys. Res.*, *99*(D11), 22,857–22,868.

Brock, C. A., F. Schröder, B. Kärcher, A. Petzold, R. Busen, and M. Fiebig (2000), Ultrafine particle size distributions measured in aircraft exhaust plumes, *J. Geophys. Res.*, *105*(D21), 26,555–26,567.

Brock, C. A., et al. (2004), Particle characteristics following cloud-modified transport from Asia to North America, *J. Geophys. Res.*, *109*, D23S26, doi:10.1029/2003JD004198, in press.

Cooper, O. R., et al. (2004), A case study of transpacific warm conveyor belt transport: Influence of merging airstreams on trace gas import to North America, *J. Geophys. Res.*, *109*, D23S08, doi:10.1029/2003JD003624, in press.

Cziczo, D. J., P. J. DeMott, C. Brock, P. K. Hudson, B. Jesse, S. M. Kreidenweis, A. J. Prenni, J. Schreiner, D. S. Thomson, and D. M. Murphy (2003), A method for single particle mass spectrometry of ice nuclei, *Aerosol Sci. Technol.*, *37*(5), 460–470.

Cziczo, D. J., D. M. Murphy, P. K. Hudson, and D. S. Thomson (2004), Single particle measurements of the chemical composition of cirrus ice residue during CRYSTAL-FACE, *J. Geophys. Res.*, *109*, D04201, doi:10.1029/2003JD004032.

de Gouw, J., C. Warneke, T. Karl, G. Eerdekens, C. van der Veen, and R. Fall (2003a), Sensitivity and specificity of atmospheric trace gas detection by proton-transfer-reaction mass spectrometry, *Int. J. Mass Spectrom.*, *223–224*, 365–382.

de Gouw, J., C. Warneke, D. D. Parrish, J. S. Holloway, M. Trainer, and F. C. Fehsenfeld (2003b), Emission sources and ocean uptake of acetonitrile (CH_3CN) in the atmosphere, *J. Geophys. Res.*, *108*(D11), 4329, doi:10.1029/2002JD002897.

de Gouw, J. A., et al. (2004), Chemical composition of air masses transported from Asia to the U.S. West Coast during ITCT 2K2: Fossil fuel combustion versus biomass-burning signatures, *J. Geophys. Res.*, *109*, D23S20, doi:10.1029/2003JD004202, in press.

Echalar, F., A. Gaudichet, H. Cachier, and P. Artaxo (1995), Aerosol emissions by tropical forest and savanna biomass-burning: Characteristic trace elements and fluxes, *Geophys. Res. Lett.*, *22*(22), 3039–3042.

Fromm, M. D., and R. Servranckx (2003), Transport of forest fires smoke above the tropopause by supercell convection, *Geophys. Res. Lett.*, *30*(10), 1542, doi:10.1029/2002GL016820.

Fromm, M., J. Alfred, K. Hoppel, J. Hornstein, R. Bevilacqua, E. Shettle, R. Servranckx, Z. Li, and B. Stocks (2000), Observations of boreal forest fire smoke in the stratosphere by POAM III, SAGE II, and lidar in 1998, *Geophys. Res. Lett.*, *27*(9), 1407–1410.

Gao, S., D. A. Hegg, P. V. Hobbs, T. W. Kirchstetter, B. I. Magi, and M. Sadilek (2003), Water-soluble organic components in aerosols associated with savanna fires in southern Africa: Identification, evolution, and distribution, *J. Geophys. Res.*, *108*(D13), 8491, doi:10.1029/2002JD002324.

Gaudichet, A., F. Echalar, J. Chatenet, J. P. Quisefit, G. Malingre, H. Cachier, P. Buat-Menard, P. Artaxo, and W. Maenhaut (1995), Trace elements in tropical African savanna biomass-burning aerosols, *J. Atmos. Chem.*, *22*, 19–39.

Guazzotti, S. A., K. R. Coffee, and K. A. Prather (2001), Continuous measurements of size-resolved particle chemistry during INDOEX-Intensive Field Phase 99, *J. Geophys. Res.*, *106*(D22), 28,607–28,627.

Guazzotti, S. A., et al. (2003), Characterization of carbonaceous aerosols outflow from India and Arabia: Biomass/biofuel burning and fossil fuel combustion, *J. Geophys. Res.*, *108*(D15), 4485, doi:10.1029/2002JD003277.

Hays, M. D., C. D. Geron, K. J. Linna, N. D. Smith, and J. J. Schauer (2002), Speciation of gas-phase and fine particle emissions from burning of foliar fuels, *Environ. Sci. Technol.*, *36*(11), 2281–2295.

Hobbs, P. V., J. S. Reid, R. A. Kotchenruther, R. J. Ferek, and R. Weiss (1997), Direct radiative forcing by smoke from biomass-burning, *Science*, *275*, 1776–1778.

Hobbs, P. V., P. Sinha, R. J. Yokelson, T. J. Christian, D. R. Blake, S. Gao, T. W. Kirchstetter, T. Novakov, and P. Pilewskie (2003), Evolution of gases and particles from a savanna fire in South Africa, *J. Geophys. Res.*, *108*(D13), 8485, doi:10.1029/2002JD002352.

Holloway, J. S., R. O. Jakoubek, D. D. Parrish, C. Gerbig, A. Volz-Thomas, S. Schmitgen, A. Fried, B. Wert, B. Henry, and J. R. Drummond (2000), Airborne intercomparison of vacuum ultraviolet fluorescence and tunable diode laser absorption measurements of tropospheric carbon monoxide, *J. Geophys. Res.*, *105*(D19), 24,251–24,261.

Holzinger, R., C. Warneke, A. Hansel, A. Jordan, W. Lindinger, D. H. Scharffe, G. Schade, and P. J. Crutzen (1999), Biomass-burning as a source of formaldehyde, acetaldehyde, methanol, acetone, acetonitrile, and hydrogen cyanide, *Geophys. Res. Lett.*, *26*(8), 1161–1164.

Ikegami, M., K. Okada, Y. Zaizen, Y. Makino, J. B. Jensen, J. L. Gras, and H. Harjanto (2001), Very high weight ratios of S/K in individual haze particles over Kalimantan during the 1997 Indonesian forest fires, *Atmos. Environ.*, *35*, 4237–4243.

Jost, H.-J., et al. (2004), In-situ observations of mid-latitude forest fire plumes deep in the stratosphere, *Geophys. Res. Lett.*, *31*, L11101, doi:10.1029/2003GL019253.

Kaufman, Y. J., and R. S. Fraser (1997), The effect of smoke particles on clouds and climate forcing, *Science*, *277*, 1636–1639.

Kirchstetter, T. W., T. Novakov, P. V. Hobbs, and B. Magi (2003), Airborne measurements of carbonaceous aerosols in southern Africa during the dry biomass-burning season, *J. Geophys. Res.*, *108*(D13), 8476, doi:10.1029/2002JD002171.

Kreidenweis, S. M., L. A. Remer, R. Bruintjes, and O. Dubovik (2001), Smoke aerosol from biomass-burning in Mexico: Hygroscopic smoke optical model, *J. Geophys. Res.*, *106*(D5), 4831–4844.

Lelieveld, J., et al. (2001), The Indian Ocean Experiment: Widespread air pollution from south and southeast Asia, *Science*, *291*, 1031–1036.

Li, J., M. Pósfai, P. V. Hobbs, and P. R. Buseck (2003), Individual aerosol particles from biomass-burning in southern Africa: 2. Compositions and aging of inorganic particles, *J. Geophys. Res.*, *108*(D13), 8484, doi:10.1029/2002JD002310.

Liu, X., P. Van Espen, F. Adams, J. Cafmeyer, and W. Maenhaut (2000), Biomass-burning in southern Africa: Individual particle characterization of atmospheric aerosols and Savanna fire samples, *J. Atmos. Chem.*, *36*, 135–155.

Loewenstein, M., H.-J. Jost, J. Grose, J. Eilers, D. Lynch, S. Jensen, and J. Marmie (2002), Argus: A new instrument for the measurement of the stratospheric dynamical tracers, N_2O and CH_4, *Spectrochim Acta A*, *58*(11), 2329–2345.

Middlebrook, A. M., et al. (2003), A comparison of particle mass spectrometers during the 1999 Atlanta Supersite Project, *J. Geophys. Res.*, *108*(D7), 8424, doi:10.1029/2001JD000660.

Mühle, J., C. A. M. Brenninkmeijer, T. S. Rhee, F. Slemr, D. E. Oram, S. A. Penkett, and A. Zahn (2002), Biomass-burning and fossil fuel signatures in the upper troposphere observed during a CARIBIC flight from Namibia to Germany, *Geophys. Res. Lett.*, *29*(19), 1910, doi:10.1029/2002GL015764.

Murphy, D. M., A. M. Middlebrook, and M. Warshawsky (2003), Cluster Analysis of Data from the Particle Analysis by Laser Mass Spectrometry (PALMS) Instrument, *Aerosol Sci. Technol.*, *37*, 382–391.

Nowak, J. B., et al. (2004), Gas-phase chemical characteristics of Asian emission plumes observed during ITCT 2K2 over the eastern North Pacific Ocean, *109*, D23S19, doi:10.1029/2003JD004488, in press.

Pósfai, M., R. Simonics, J. Li, P. V. Hobbs, and P. R. Buseck (2003), Individual aerosol particles from biomass-burning in southern Africa: 1. Compositions and size distributions of carbonaceous particles, *J. Geophys. Res.*, *108*(D13), 8483, doi:10.1029/2002JD002291.

Proffitt, M. H., and R. J. McLaughlin (1983), Fast-response dual-beam UV-absorption ozone photometer suitable for use on stratospheric balloons, *Rev. Sci. Instrum.*, *54*(12), 1719–1728.

Schreiner, J., U. Schild, C. Voigt, and K. Mauersberger (1999), Focusing of aerosols into a particle beam at pressures from 10 to 150 Torr, *Aerosol Sci. Technol.*, *31*(5), 373–382.

Sheesley, R. J., J. J. Schauer, Z. Chowdury, G. R. Cass, and B. R. T. Simoneit (2003), Characterization of organic aerosols emitted from the combustion of biomass indigenous to South Asia, *J. Geophys. Res.*, *108*(D9), 4285, doi:10.1029/2002JD002981.

Silva, P. J., D.-Y. Liu, C. A. Noble, and K. A. Prather (1999), Size and Chemical Characterization of Individual Particles Resulting from Biomass-burning of Local Southern California Species, *Environ. Sci. Technol.*, *33*(18), 3068–3076.

Singh, H. B., et al. (2003), In situ measurements of HCN and CH_3CN over the Pacific Ocean: Sources, sinks, and budgets, *J. Geophys. Res.*, *108*(D20), 8795, doi:10.1029/2002JD003006.

Sinha, P., P. V. Hobbs, R. J. Yokelson, I. T. Bertschi, D. R. Blake, I. J. Simpson, S. Gao, T. W. Kirchstetter, and T. Novakov (2003), Emissions of trace gases and particles from savanna fires in southern Africa, *J. Geophys. Res.*, *108*(D13), 8487, doi:10.1029/2002JD002325.

Thomson, D. S., M. E. Schein, and D. M. Murphy (2000), Particle analysis by laser mass spectrometry WB-57F instrument overview, *Aerosol Sci. Technol.*, *33*, 153–169.

Warneke, C., J. A. de Gouw, D. D. Parrish, J. S. Holloway, T. B. Ryerson, D. K. Nicks Jr., M. Trainer, and F. Fehsenfeld (2002), Enhancement of VOCs in a fresh and an aged forest fire plume, *Eos Trans. AGU*, *83*(47), Fall Meet. Suppl., Abstract A62B-0161.

D. J. Cziczo, J. A. de Gouw, J. Holloway, G. Hübler, P. K. Hudson, D. M. Murphy, D. S. Thomson, and C. Warneke, NOAA Aeronomy Lab, Boulder, CO 80305, USA. (phudson@al.noaa.gov)

H.-J. Jost, Bay Area Environmental Research Institute, Sonoma, CA 95476, USA.